Jour. Fac. Sci., Hokkaido Univ., Ser. VII (Geophysics), Vol. 9, No. 1, 1-16, 1991.

An Estimate of the Velocity and Stress in the Deep Ocean Bottom Boundary Layer

Sei-ichi Kanari, Chikashi Kobayashi

Department of Geophysics, Faculty of Science, Hokkaido University, Sapporo 060, Japan

and

Takayuki Ishikawa

Institute of Low Temperature Science, Hokkaido University, Sapporo 060, Japan

(Received July 21, 1990)

Abstract

In order to estimate the near-bottom velocity and the boundary shear stress, a one-dimensional unsteady boundary layer model was applied for the observed time series of the 6-level current observation conducted from Oct. 26 through to Nov. 3, 1988 at the site of the north western end of the Kyushu-Palau Ridge. Current meters were deployed 6, 10.5, 18.5, 39.0, 75.0 and 151.0 meters respectively up from the sea floor of 3519 m depth for seven days. The applied model, developed by McLean and Yean, predicts fairly well the near-bottom velocity field and stress, with the adjusted roughness of $z_0=0.025$ cm. The estimated time-averaged drag coefficient is 4.5×10^{-3}. Thickness of the logarithmic layer is inferred as the order of 1 meter, which overlies the viscous sublayer of a thickness of about 1 cm.

1. Introduction

In recent observations of salinity and potential temperature taken at the bottom of the deep ocean, profiles often exhibit a well-mixed region just above the bottom, which is often referred to as the benthic boundary layer (Weatherly and Kelley, 1982; Armi and Millard, 1976). The thickness of the benthic boundary layer (hereafter referred to as BBL) varies in time and space, and the thickness extends from ten meters to a hundred meters. Armi and Millard (1976) have correlated the thickness of the BBL with the velocity observed in a water column above the layer, and showed that the BBL thickness in the Hatteras Abyssal Plain extending above the bottom to about 6 times the turbu-

lent Ekman layer height.

Weatherly and Kelley (1982) have examined near-bottom CTD data and current meter records obtained on the continental rise south of Nova Scotia, and found that the bottom layer of thickness of about 60 m is part of a continuous ribbon or filament with a width of about 100 km (they referred to this feature as the Cold Filament) found on the continental margin near its base, and the Cold Filament is a distinct layer of water flowing along the bottom with a thickness comparable to that associated with bottom mixed layers.

Our main interest is in understanding of the physical process associated with the variations of the thickness of BBL. We are also expecting that the Cold Filament theory is one of the major processes associated with the variations of bottom mixed layers. In order to clarify the physical processes and its mechanism near the deep ocean bottom as mentioned above, two sets of 6-levels current meter system have been moored at different sites. One is at the site of 3519 m depths of north western end of Kyushu- Palau Ridge (referred as KPR in Fig. 1.), and the other is at the site of 4,540 m depths of north western end of

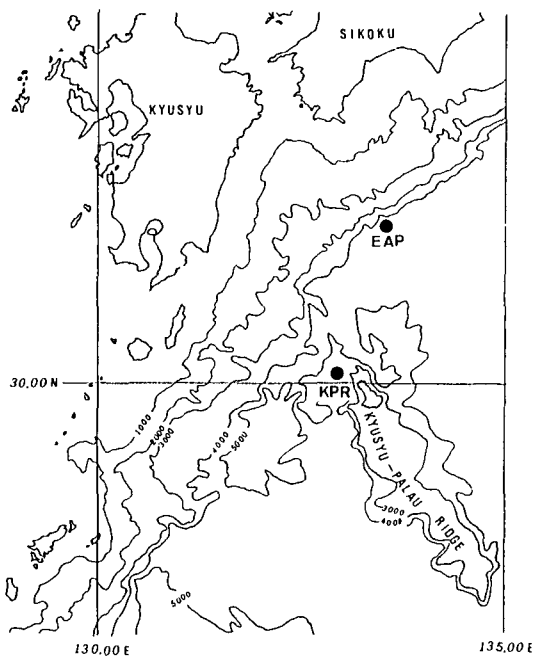

Fig. 1. Topographic map of the north western part of Shikoku Basin. Locations of mooring site are indicated by the solid circles. Depths are in meters.

Abyssal Plain in Shikoku Basin (referred as EAP in Fig. 1.) as shown in Fig. 1. The system at KPR was moored between 26 October 1988 and 3 November 1988 as a preliminary observation, and the system at EAP was moored on 19 September 1989 and is under operation (this system is expected to be retrieved in September 1990).

In the present study, preliminary current data at KPR was examined using a one-dimensional, time-dependent model as described by McLean and Yean (1987).

2. Description of the mooring system

For the pupose of near-bottom observation, compact-sized electro-magnetic current meters (ACM-5000S), which has bean newly developed by Alec Electronics Co., were adopted. The Current meter, length 50 cm, 9 cm diameter, 15 kg weight in water has a maximum operating depth of 5,000 m. The instrument has a two axes electro-magnetic type velocity sentor and a temperature sensor with a range from -2 to $+12$°C with an accuracy of ± 0.01°C (resolution of 0.005°C), which could possibly measure weak temperature changes in the deep ocean.

In the current observation at the site of KPR, every data sampling scheme used was 100 samples in a burst every 10 minutes. As shown in Fig. 2, six current meters were deployed vertically with an equal interval in logarithmic vertical scale. The current meter sensors were positioned at 6 m, 10.5 m, 18.5 m, 39 m, 75 m and 151 m respectively above the bottom.

3. Current meter data

Observed time series of current vectors are shown in Fig. 3. The time series of current vector at respective layer is dominated with M_2 component of tides and inertial period oscillation. The maximum velocity of composed current vector of those two major components reaches about 15 cm/s, while the mean velocity is less than 2 cm/s to the NE.

Fig. 4 shows the mean velocity profile. The magnitude of the flow is almost constant above the height of 39 m, but gradually decreases below it to the bottom. The dashed line in Fig. 4 represents a presumed profile, and it suggests that the thickness of BBL is less than 39 m.

Temperature data of respective current meter showed a constant temperature of 1.55°C through the whole layer, and we concluded that there was no

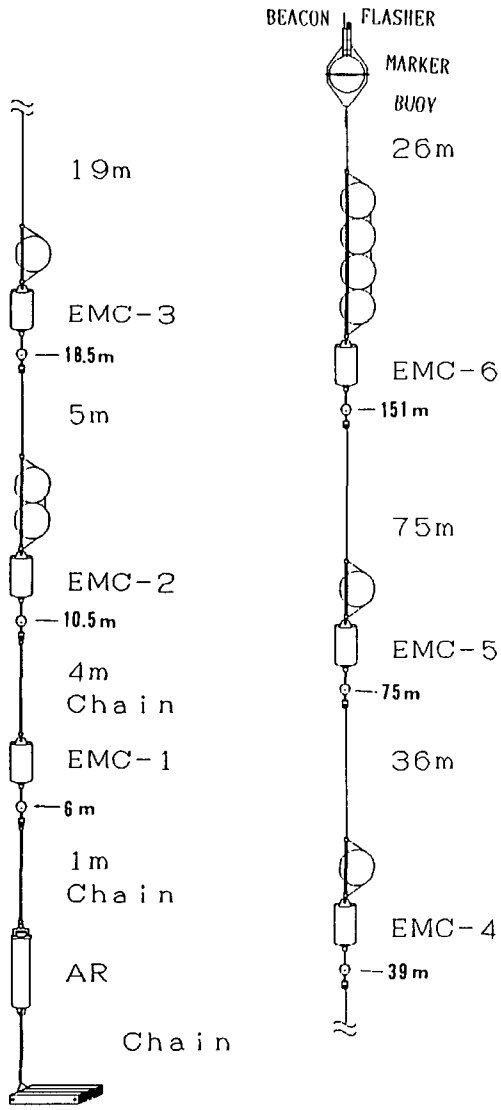

Fig. 2. Structure of current meter mooring system.

significant thermal stratification between the toplayer and bottom.

The thickness of bottom Ekman layer is given by a friction depth when eddy viscosity is constant. Wimbush and Munk (1971), and Weatherly (1972, 1975) have mentioned that the thickness of turbulent Ekman layer can be given by the

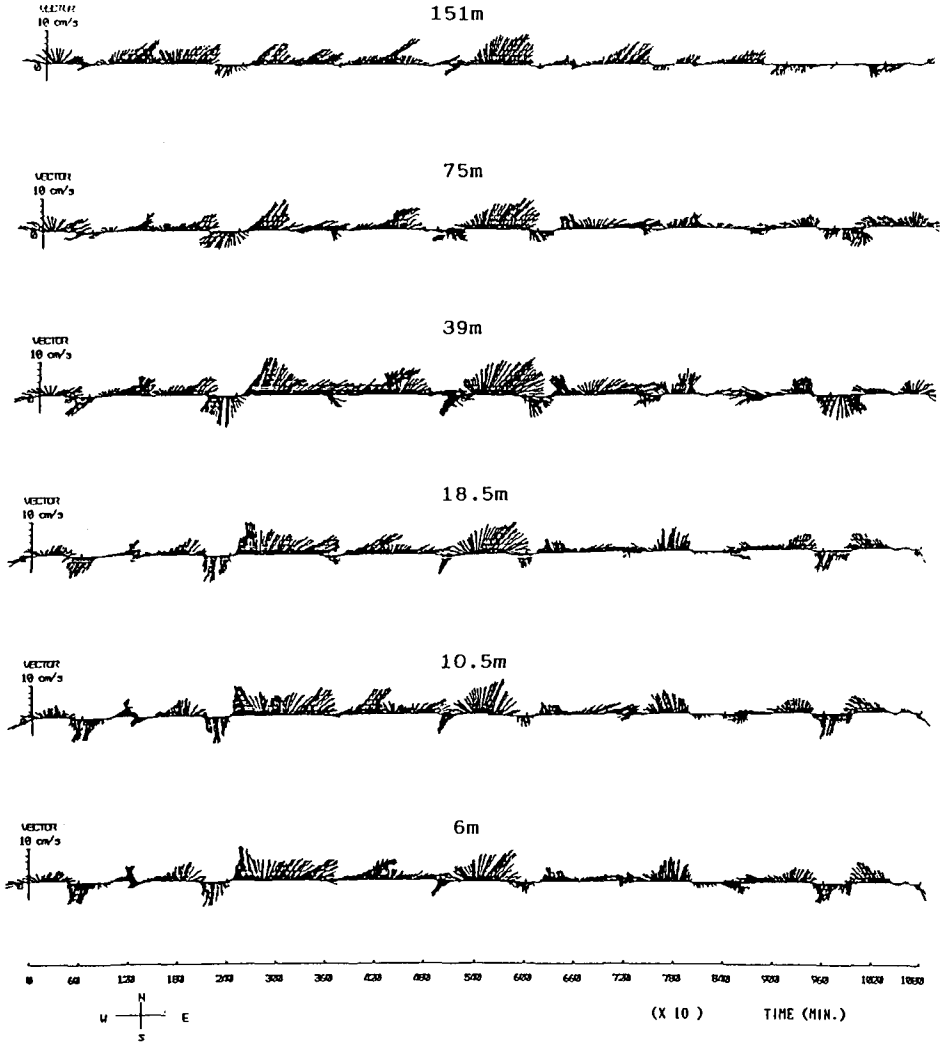

Fig. 3. Observed time series of current vector at 151 m, 75 m, 39 m, 18.5 m, 10.5 m, and 6 m above the sea floor. The figures below the horizontal axis show the data number at every ten minutes intervals.

friction depth derived by Ekman theory. For the depth and time-dependent eddy viscosity, the friction depth can mot be expected to give a reasonable thickness of the bottom boundary layer. Based on the laboratory experiments, Caldwell et al. (1972), and also Howroyed and Slawson (1975) have presented the thickness of turbulent bottom Ekman layer h_e as follows,

$$h_e = 0.4 u_* / f \tag{1}$$

where, u_* is the friction velocity, and $f = 2\omega \sin \varphi$ is Coriolis parameter. Biscaye and Eittreim (1974) have empirically estimated the friction velocity as 1/30 of a representative velocity.

In the present case, replacing the root mean square of the velocity in the

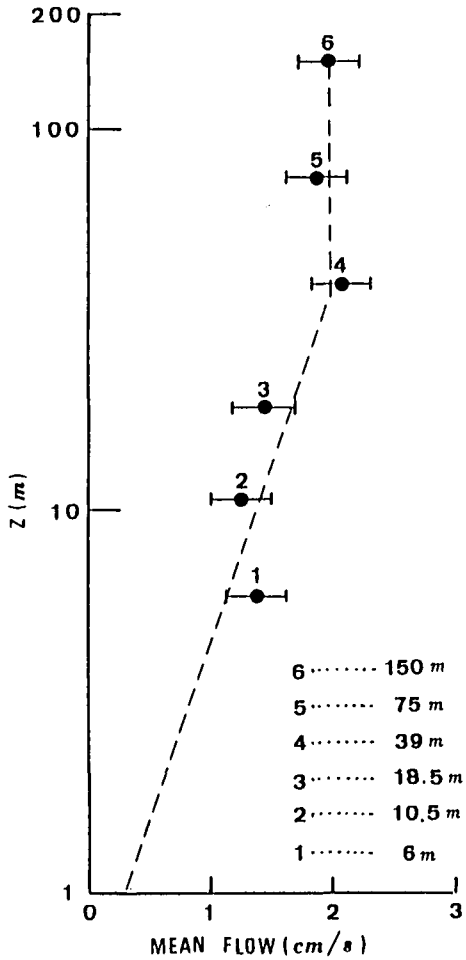

Fig. 4. The vertical profile of time averaged mean flow. The horizontal lines show the probable error of current measurement. The dashed line shows the presumed mean flow profile.

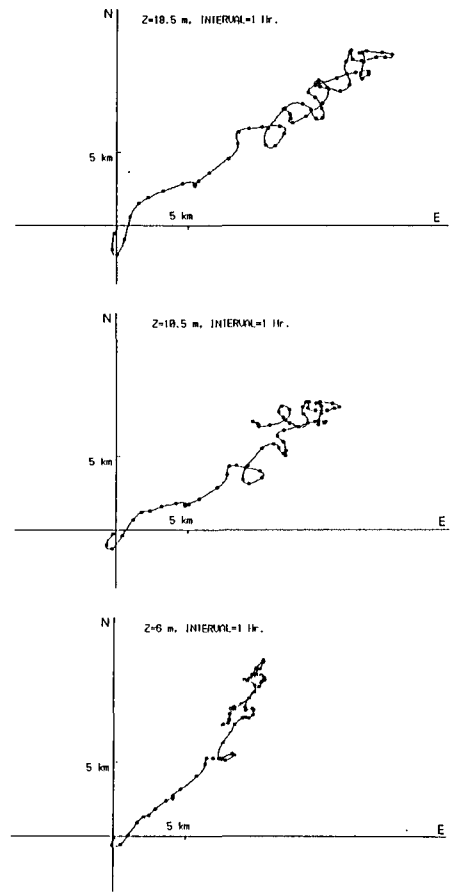

Fig. 5. Progressive vector diagrams based on the lower three current meters.

present time series as a representative velocity, the thickness of the bottom Ekman boundary layer is estimated as 29 m, which is not quite inconsistent with the boundary height inferred from the mean profile as given in Fig. 4.

As seen in Fig. 5. the progressive vector of the flow of lower three layers show a tendency of anticlockwise bearing of flow direction with the decreasing height. The bearing angle of the progressive vectors between 6 m-layer and 10.5 m-layer is about 6° on an average.

4. Bottom boundary layer model

Assuming a horizontally uniform flow, linear balance of the horizontal flow in the x, iy, z coordinate can be expressed by the following form,

$$\partial t q(t, z)+ifq\ (t, z)=\rho^{-1}\ (\partial_n P(t, z)+\partial_z \tau(t, z)) \tag{2}$$

where, $q=u+iv$, $\tau=\tau_x+i\tau_y$, $\partial_m=\partial/\partial_m$ is an operator of partial derivative, $\partial_n P=\partial_x P+i\partial y P$, and $i=\sqrt{-1}$.

Further, assuming a quasi-geostrophic balance outside the BBL, the current field above the boundary can be given by

$$\partial_t q_G+ifq_G=-\rho^{-1}\partial_n P \tag{3}$$

where, $q_G=v_G+iv_G$ is a quasi-geostrophic current.

Eliminating the pressure term using (2) and (3), we have

$$\partial_z \tau(t, z)=(\partial_t+jf)(q_G(t, h)-q(t, z)) \tag{4}$$

The shear stress in a flow field with eddy viscosity ν is given by

$$\tau(t, z)=\nu\partial_z q\ (t, z) \tag{5}$$

Using (4) and (5), one can estimate the internal shear stress and flow field alternately with the finite difference method, if the eddy coefficient is *a priori* given.

After McLean and Yean (1987), we adopted the form of eddy viscosity ν_e for channel flow, given by Long (1981), that is, $\nu=\nu_e+\nu_m$ and

$$\nu_e=ku_*(t, z)\ z\cdot\exp(-zf/0.6u_*(t, z)) \tag{6}$$

where, ν_m is the molecular viscosity, k is karman's constant given by 0.4, z is the height above the bottom.

In the present model, we assumed the layer of 39 m is just above the BBL, and adopted the time series of flow velocity at 39 m level as $q_G\ (t, h)$.

Time integration from (4) to (5) with (6) was carried out by a finite

difference scheme in the frequency domain on the Fourier transformed quantities, $\tau^*(\omega, z)$, $q^*(\omega, z)$ and $q_G^*(\omega, z)$. The vertical grid size Δz for the difference scheme was selected such that the vertical grid has equal intervals on the logarithmic scale. For this, the vertical axis z was transformed to ξ axis using the following form.

$$\xi = \ln(z/z_0)/\ln(h/z_0) \tag{7}$$

where, z_0 is a roughness parameter, h is the thickness of BBL, assuming $h=39$ m. The transformation leads to

$$\Delta z = \lambda z \Delta \xi \tag{8}$$

where, $\lambda = 1/1.443\ln(h/z_0)$.

Thus, the fourier transformed stress for the $j+\frac{1}{2}$ layer can be calculated with the stress at the level of j and with the flow velocities $q_G^*(\omega, h)$ and $q^*(\omega, j+1)$ using the following finite difference form.

$$\tau^*\left(\omega, j+\frac{1}{2}\right) = \tau^*\left(\omega, j-\frac{1}{2}\right) + i(\omega+f)\Delta z\left\{q^*(\omega, j) - q_G^*(\omega, h)\right\} \tag{9}$$

The level $j=1$ corresponds to the level just below the boundary, where the stress $\tau^*(\omega, j)$ is assumed as $\tau^*(\omega, \frac{1}{2})=0$. The flow relocity $q^*(\omega, 2)$ can be given by the Fourier transform of the measured time series at the height of 18.5 m above the bottom.

The finite difference form of equation (5) for the grids of $j+1$ and $j+2$ gives the prediction of flow at $j+2$, that is

$$q(j+2) = q(j+1) - \Delta z \cdot \tau(j+1)/\nu(j+1) \tag{10}$$

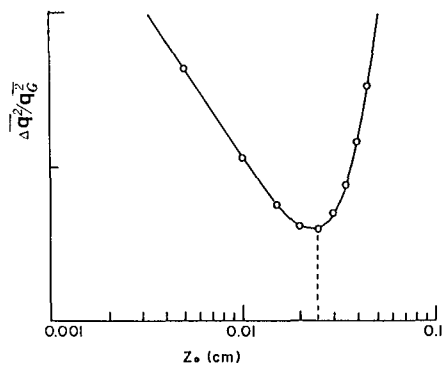

Fig. 6. Relative change of the root-mean square error of velocity between the observed and estimated flow against the roughness parameter z_o. The vertical dashed line shows the optimum value of z_o, adopted in the calculation described in the text.

where, $\tau\left(t, j+\frac{1}{2}\right)$ is the stress time series given by the inverse transform of eq. (9).

The boundary condition at the bottom becomes

$$q(t, z)=0 \text{ at } z=z_0 \tag{11}$$

To carry out the above successive calculation, the roughness parameter z_0 must be previously determined. As a result of trials for various values of z_0, we found that the fraction of r.m.s. error between the observed time series of currents and estimated one becomes minimum at a certain z_0-value, and we selected the value of $z_0=0.025$ cm with the minimum fraction as shown in Fig. 6.

5. Estimated flow and stress

The result of flow estimation at the height of 6 m is shown in the lower in Fig. 7 comparable to the observed vector time series in the same figure (upper). Fig. 8 shows the result of further estimates at the heights from 3 m to 9.375 cm, though there are no observed data to compare. The flow velocity gradually decreases as close to the bottom floor, but change of the bearing angle of the flow does not seem to be so significant.

An example of the estimated time series of stress components, and corresponding parameters at the height of 14 cm are shown in Fig. 9. The time series of drag coefficient C_d is calculated from the time series of absolute stress $|T|$ divided by the r.m.s. quasi-geostrophic current velocity $\langle q_G \rangle$. The time average of C_d is about 0.0045. However, the large amount of variability ranges

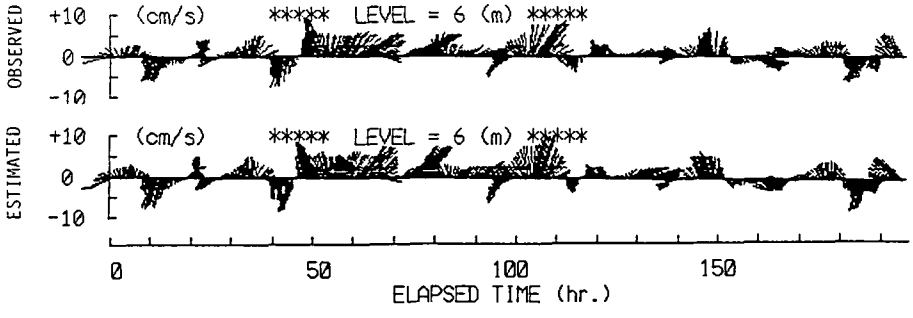

Fig. 7. Time series of velocity vector at 6 m above the bottom. Observed velocity vector (a), and estimated (b).

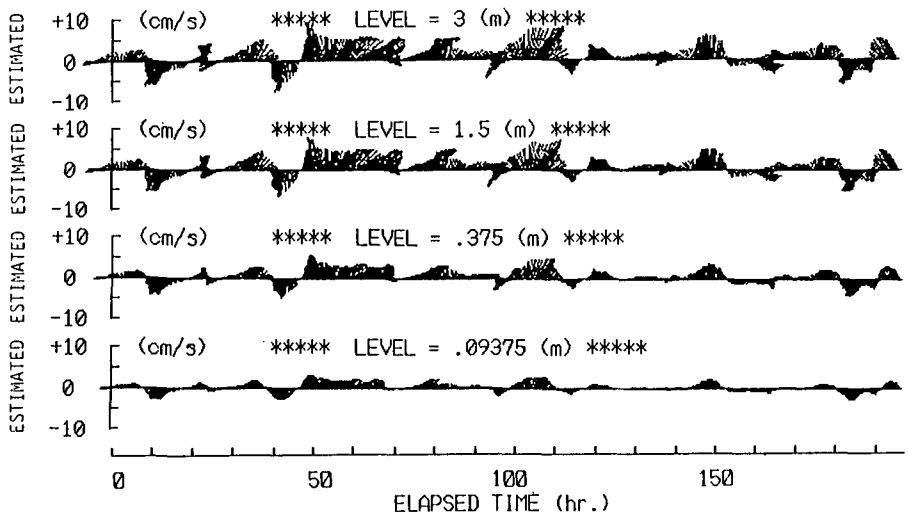

Fig. 8. Estimated time series of current vector at 3 m, 1.5 m, 0.375 m, and 0.094 m above the bottom respectively.

from 10^{-4} to 0.008. McLean and Yean (1987) have suggested that such a wild fluctuation of C_d is attributable to the low flow velocity outside frictional layer.

The time series, denoted by P_h which is the bottom line in the same figure shows the bearing angle between the flow vector and stress vector $-\tau$ rotated by 180°. Accordingly, the line of $P_h=0$ means that the vector of bottom stress acting in the opposing direction to the outside flow. Though the total time length of the opposed stress vectors is only about 40% of the time span at the height of 14 cm, the fraction increases to more than 90% within the viscous sublayer of thickness of about 1 cm, as shown in Fig. 10.

There can be seen intermittent large fluctuations of the deflection angle in the respective time series of P_h. The angle P_h near $\pm 180°$ means that the stress vector is acting in the same direction of outside flow, and that in such case, the stress locally accelerates the fluid on the sea floor. The duration time of such an intermittent fluctuation becomes shorter with the decreasing height from the bottom, and the feature seems to suggest the "Turbulent burst" event.

The vertical profiles of the time averaged viscosity, stress, friction velocity, and drag coefficient are shown in Fig. 11. As seen from the assumed form, the viscosity reaches its maximum (80 cm^2/s) at 10 m above the bottom and tends to be its minimum (0.01 cm^2/s) below it. The stress, friction velocity, and therefore the drag coefficient gradually increases from the upper boundary, and

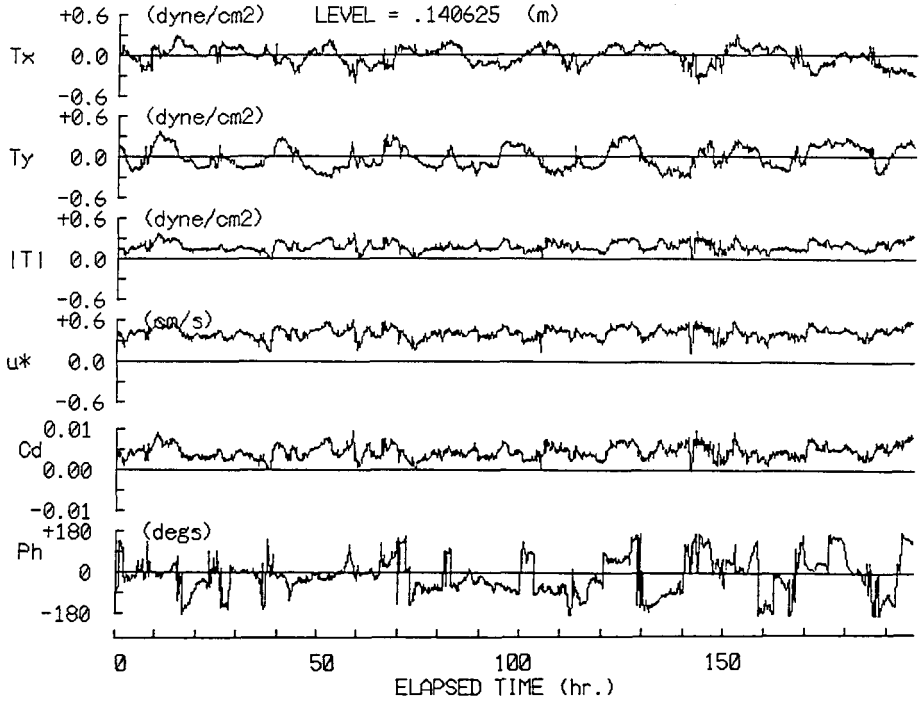

Fig. 9. Estimated time series of near bottom ($z=0.14$ m) shear stress components T_x, T_y, magnitude of stress $|T|$, friction velocity u_*, drag coefficient C_d, and the bearing angle of stress vector P_h against the guasi-geostrophic current vector outside the Ekman boundary layer. The angle P_h is measured with rotating the stress vector by 180°.

become almost constant below the height of 1 m, which corresponds to the constant stress bottom boundary layer with logarithmic velocity profile.

6. Viscous sublayer

As seen in Fig. 8, there remains a considerable flow velocity of 3 cm/s even at 9 cm above the bottom. The vertical profile of stress in Fig. 11 suggests a logarithmic profile of flow at the level below 1 m.

Estimated vertical structure of the fourier amplitude velocity for the three components of the inertial, the semidiurnal, and the mean are plotted in Fig. 12. As presumed in Fig. 11, each profile shows a logarithmic velocity distribution between the height of 3 m and 0.01 m above the bottom.

At the height from 0.01 m to z_0, the flow velocity deviates from the line of

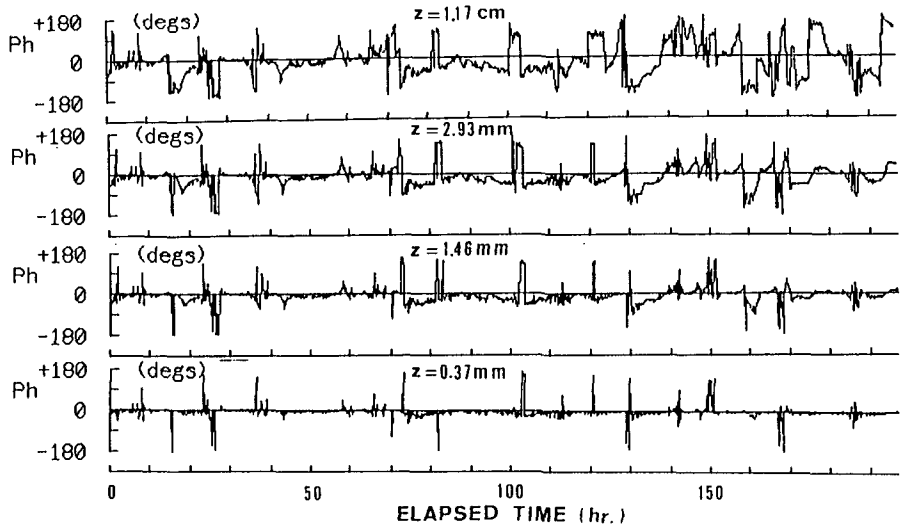

Fig. 10. Variations of the bearing angle P_h within the viscous sub-layer. At 0.37 mm above the bottom, the stress vector becomes to be in the opposed direction to the outside flow except that the large angle at the intermittent burstlike events of short time duration.

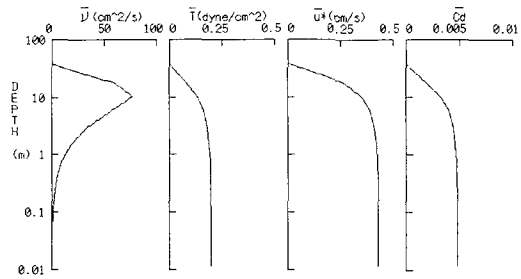

Fig. 11. Time averaged vertical profiles of turbulent parameters within the assumed Ekman boundary layer.

log-profile and approaches zero at z_0.

Chriss and Caldwell (1984) have discussed the observed profile of near bottom flow over the slope of continental shelf off Oregon Coast, and concluded that the thickness of the viscous sublayer of flow, deviating from log-profile, is about 1 cm.

Denoting the thickness of viscous sublayer as δ, the velocity profile of logarithmic layer can be given by

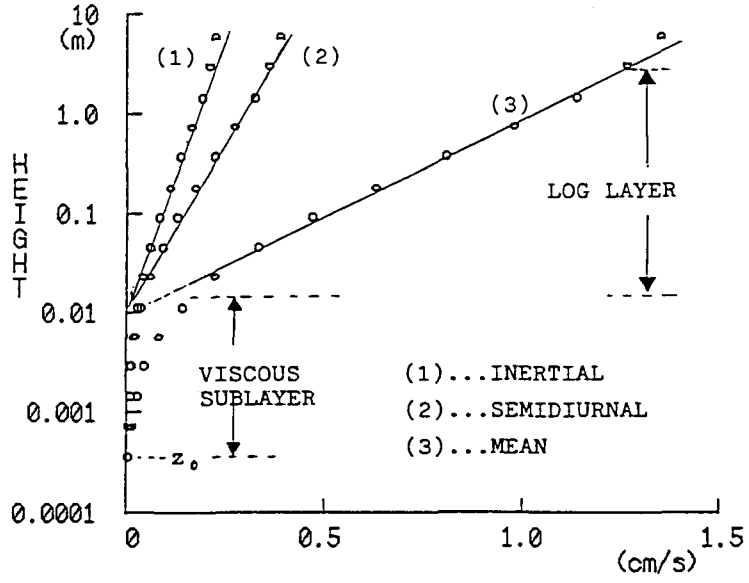

Fig. 12. Vertical structure of the Fourier amplitude velocity for the inertial (1), the semidiurnal (2), and the mean (3) components respectively within a logarithmic layer and viscous sublayer.

$$u(z)=\frac{u_*}{k}\ln(z)+C \tag{12}$$

where C is constant.

Assuming a constant viscosity ($\nu=\nu_c$) and friction velocity, the flow velocity in the viscous sublayer can be simply written with another constant C' as

$$u(z)=\frac{{u_*}^2}{\nu_c}z+C' \tag{13}$$

As the flow must be continuous at $z=\delta$, then, from (12) and (13), we have

$$C-C'=\frac{u_*}{\nu_c}\delta-\frac{u_*}{k}\ln(\delta) \tag{14}$$

No flow condition at $z=z_0$ leads to

$$C'\equiv\frac{{u_*}^2}{\nu_c}z_0 \tag{15}$$

From (12) to (15), the velocity profiles in respective layer can be given as follows.

$$\bar{u}(z)=\frac{u_*}{k}\ln\left(\frac{z}{\delta}\right)+\frac{{u_*}^2}{\nu_c}(\delta-z_0);\ \delta\leq z\leq\delta_l \tag{16}$$

and

$$\bar{u}(z)=\frac{{u_*}^2}{\nu_c}(z-z_0);\ z_0\leq z<\delta \tag{17}$$

Where, δ_l is the thickness of the log-layer.

Fitting eq. (17) to the mean flow in the sublayer in Fig. 12 leads to the constant viscosity of 1.2 cm^2/s.

7. Conclusion

Structure of the near bottom flow and boundary shear stress were estimated from the measured time series of currents, using a time dependent linear bottom boundary layer model described by McLean and Yean (1987). The thickness of bottom boundary layer inferred from the mean current profile nearly corresponds to that given by eq. (1).

Calculation by the present scheme is required to give the value of z_0 *a priori*. The value of z_0 was determined by an iterative least square method, so that the r.m.s. of the difference between the estimated time series of the flow and measured one at the lowest height (6 m) becomes minimum at a certain z_0-value. The determined z_0-value was 0.025 cm.

Following McLean and Yean (1987), we adopted the Long's eddy viscosity formula with the length scale of 0.44 u_*/f, but we used it in the form of Long's formula plus molecular viscosity.

The scheme described above is certainly available for estimation of the flow and stress in the bottom boundary layer (BBL) if the thickness of BBL has been properly determined. In the present data, the thickness, derived from mean velocity profile is consistent with the turbulent Ekman height, given by $h=0.4\ u_*/f$.

Since the time averaged friction velocity is 0.4 cm/s the bottom surface the Rossby number u_*/fz_0 becomes 2.22×10^5. The result of calculation shows that the log-layer thickness begins at 3 m above the bottom. The resultant thickness of log-layer almost coincides with the thickness given by $\delta_l=0.057\ u_*/f$, accordingly the data point of the nodimensionalized log-layer thickness δ_l/z_0 versus surface Rossby number u_*/fz_0 was very close to the line given by $\delta_l=0.057\ u_*/f$ which was presented by Lavelle and Mofjeld (1983).

The eddy viscosity assumed in the calculation decreases almost exponential-

ly within the log-layer and becomes almost constant value, represented by additional molecular viscosity term, at the height of about 1 cm above the sea floor ($z=z_0$). Below this height, the time averaged velocity profiles deviate significantly from the logarithmic profile. It is suggestive that the thin non-logarithmic layer with the thickness of about 1 cm corresponds to the viscous sublayer described by Chriss and Caldwell (1984).

In this paper, we could not deal with the variations of the boundary layer thickness. Such arguments will be given in future using the long-term mooring data at the site EAP which is now under operation.

Acknowledgments

The author thanks many scientific and operational crew, who were engaged in the cruise of KE-89-11 carried out by T/V KEITEN-MARU of Kagoshima University, for their cooperation and help to cast and recovery of the mooring system.

The author also thanks Dr. T. Teramoto who were the director of the Research Program on the Dynamics of the Deep Ocean Circulation, who gave us a chance and encouragements for the present study.

We are also indebted to Dr. M. Chaen of Kagoshima University for his help in arranging the navigation, and management of the field operation throughout the program.

This work was supported by a Grant-in-Aid No. 0160008 for Scientific Research of the Priority Area Program, the Dynamics of the Deep Ocean Circulation by the Ministry of Education, Science and Culture of Japan, and this support is gratefully acknowledged.

References

Armi L. and R.C. Millard, 1976. The bottom boundary layer of the ocean. J. Geophys., Res., **81**, 4983-4990.

Biscaye P.E. and S.L. Eittreim, 1974. Variation in benthic boundary layer phenomena: Nepheloid layer in the North Atlantic Basin, in Suspended Solids in Water (ed) R.J. Gibbs, Plenum, New York, 227-260.

Caldwell D.R., L. W. Van Atta and K.N. Helland, 1972. A laboratory study of the turbulent Ekman layer. Geophys. Fluid Dyn., **3**, 125-160.

Chriss T.M. and D.R. Caldwell, 1984. Universal similarity and the thickness of the viscous sublayer at the ocean floor. J. Geophys. Res., **89**, 6403-6414.

Howroyed G.C. and P. R. Slawson, 1975. The characeristics of a laboratory produced turbulent Ekman layer. Boundary Layer Met., **8**, 201-219.

Lavelle J.W. and H.O. Mofjeld, 1983. Effects of time-varying viscosity on oscillatory turbu-

lent channel flow. J. Geophys. Res., **88**, 7607-7616.
Long C.E., 1981. A simple model for time-dependent stably stratified turbulent boundary layers. Ref. M81-04, Dept. of Oceanogr., University of Washington, 170 pp.
McLean S. R. and J. Yean, 1987. Velocity and stress in the deep-ocean boundary layer. J. Phys. Oceanogr., **17**, 1356-1365.
Weatherly G., 1972. A study of the bottom boundary layer of the florida Current. J. Phys. Oceanogr., **2**, 54-72.
Weatherly G., 1975. A numerical study of time-dependent turbulent Ekman layers over horizontal and sloping bottoms. J. Phys. Oceanogr., **5**, 288-299.
Weatherly G.L. and E.A. Kelley Jr., 1987. 'Too cold' bottom layers at the base of the Scotian Rise. J. Mar, Res., **40**, 985-1012.
Wimbush M. and W. Munk, 1970. The benthic boundary layer. The Sea, 4, **1**, John Wiley, New York, 731-758.